Endocytic dynamin deficiency impairs the host colonization of phytopathogenic fungi

Xin Chen[1,2], Xiaomin Chen[3], Yunfei Long[1,2], Zhenyu Fang[1,2], Yakubu Saddeeq Abubakar[1,5], Huawei Zheng[4], Zonghua Wang[1,4*], Wenhui Zheng[1,2*]

[1] State Key Laboratory for Ecological Pest Control of Fujian and Taiwan Crops, College of Plant Protection, Fujian Agriculture and Forestry University, Fuzhou, 350000 China;

[2] Key Laboratory of Bio-pesticide and Chemical Biology, Ministry of Education, College of Plant Protection, Fujian Agriculture and Forestry University, Fuzhou, 350000 China;

[3] Fujian University Key Laboratory for Plant Microbe Interaction, College of Life Sciences, Fujian Agriculture and Forestry University, Fuzhou 350002, China;

[4] Ministerial and Provincial Joint Innovation Centre for Safety Production of Cross-Strait Crops, College of Geography and Oceanography, Minjiang University, Fuzhou 350108, China;

[5] Department of Biochemistry, Faculty of Life Science, Ahmadu Bello University, Zaria 810281, Nigeria.

* Authors for correspondence:

Wenhui Zheng (wenhuiz@fafu.edu.cn), Zonghua Wang (wangzh@fafu.edu.cn).

Abstract

During host-pathogen interactions, pathogens employ endolysosomal trafficking to fine-tune host and environmental cues, facilitating disease progression. Inhibiting the functions of the endolysosomal network could be promising for the control of plant fungal diseases. Herein, we showed that inhibition of the endocytic dynamin FgVps1 by the phenothiazines chlorpromazine (CPZ) and prochlorperazine (PCZ) leads to endolysosomal dysfunction. Further analyses revealed that the phenothiazines directly bind the GTPase domain of FgVps1 to inhibit its activity. Moreover, our results showed that FgVps1 is recruited to the endosome by the Rab GTPases FgRab51 and FgRab7 to facilitate the release of retromer- and sorting nexin-coated vesicles, thereby ensuring the proper recycling of some cargos and promoting fungal development and pathogenicity. Direct treatment of the phytopathogens *F. graminearum*, *Magnaporthe oryzae* and *Fusarium oxysporum f. sp. cubense* with CPZ and PCZ also impairs their growth, development and virulence. These results unveil the underlying mechanisms of endocytic dynamin actions and provide a potential strategy for broad-spectrum control of phytopathogenic fungi.

Key words

endocytic trafficking, dynamin, Rab GTPase, sorting machinery, phenothiazines, phytopathogenic fungi

Introduction

Each year, crop losses caused by emerging fungal pathogens pose a seriously risk to global food security [1, 2]. The progression of these diseases depends on the complex interplay between environmental factors, hosts and pathogens [3, 4]. Understanding the multicellular strategies that pathogens use to maintain homeostasis and adapt to environmental conditions during interactions with hosts will enhance our knowledge of disease development and lead to more effective control strategies.

The maintenance of cellular homeostasis when exposed to biotic and abiotic stresses is spatiotemporally controlled by the endolysosomal network in eukaryotes [5]. Cell surface cargo proteins entry the endolysosomal network following endocytosis and reach the early endosomes

where cargo sorting is initiated. At the early endosome, the fates of the cargos are decided: to be recycled or degraded [5, 6]. For recycling, cargo proteins can be directly delivered to the cell surface or transit through the endocytic recycle compartment to be delivered to the cell surface. In addition, some selected cargo proteins can be retrieved into the trans-Golgi by the retromer complex for subsequent delivery to the cell surface through the secretory pathway. For degradation, cargo proteins at the late endosome are sorted into the multivesicular body (MVB) which further fuses with the vacuole to empty its contents for degradation. This is fine-tuned by Rab GTPases, PIPs and ESCRT machinery [6, 7, 8].

Highlighting its importance, the endolysosomal network is associated with the pathogenesis of plant pathogenic fungi. Dysfunction of the endolysosomal network impairs the vegetative growth and infection-related development of various fungal pathogens [9, 10, 11, 12, 13, 14, 15, 16, 17, 18, 19, 20, 21, 22, 23, 24, 25, 26, 27, 28, 29, 30]. Additionally, the endolysosomal network is required for effective modulation of autophagy process, which helps in adaptation to metabolic changes and environmental cues during pathogen-host interactions[21, 26, 27, 28, 29]. To suppress host immune responses, fungal pathogens use the endolysosomal network to facilitate secretion of effector proteins during host infection [14]. Furthermore, the endolysosomal network is highly linked with mycotoxin production, the toxic secondary metabolites that seriously threaten food security and animal health but are useful for host colonization [10, 11, 12, 13, 23, 24, 25, 31]. Given the accumulating evidence showing the important roles of the endolysosomal network in the pathogenesis of fungal phytopathogens, we hypothesized that disrupting the endolysosomal network might have potential applications in fungal disease control.

Endocytosis, the beginning of the endolysosomal network, governs the internalization of cargo proteins and molecules and has shown its potential in clinical treatment of various diseases [32, 33, 34, 35]. Among the various endocytosis pathways identified, clathrin-mediated endocytosis (CME) is the major and well-characterized endocytic pathway [33, 36, 37]. Briefly, adaptor protein-2 binds a cargo protein from one end and binds clathrin at the other end to initiate the assembly of clathrin-coated pits (CCP). Other adaptors are then recruited to the CCP to ensure its stabilization and maturation. After maturation, dynamins drive the scission of the clathrin-coated vesicle to allow for internalization and subsequent fusion of the vesicle with early endosome [33, 36, 37]. In addition to

mediating the release of the clathrin-coated vesicle, dynamins also participate in membrane remodeling events during vesicle trafficking [38, 39]. However, whether antifungal agents exert their functions by targeting endocytic dynamins remains largely unknown.

In the present study, we evaluated the mechanistic relationship between phenothiazines (a class of endocytosis inhibitors) and the activity of the dynamin Vps1 [34, 40]. Treatment with phenothiazines significantly impairs the development and virulence of phytopathogenic fungi. We also found that phenothiazines target FgVps1 and inhibit its GTPase activity via binding to its G domain region, consequently disrupting endocytosis process in *F. graminearum*. Furthermore, FgVps1 is recruited to the endosome by the Rab GTPases FgRab51 and FgRab7 to facilitate endocytic trafficking by mediating the scission of retromer- and sorting nexins-coated endosomal tubules. Moreover, FgSnc1 is identified as the cargo protein in FgVps1-associated endocytic trafficking, and its intracellular trafficking requires the GTPase activity of FgVps1. These results provide insight into the complex interplay of the endolysosomal network in pathogenic fungi and highlight the potentials of phenothiazines for the control of phytopathogenic fungal diseases.

Results

Phenothiazines impair the development and pathogenicity of fungal pathogens

Previously, we highlighted the important roles of endolysosomal network in the development and pathogenicity of *F. graminearum*, the causal agent of wheat head blight [9, 10, 11, 12, 23, 24, 25, 41]. Since the endolysosmal network begins with endocytosis of surface cargos, inhibition of endocytosis could impair the homeostasis of the network. Phenothiazines have previously been shown to inhibit endocytosis in mammals [5, 34, 40, 42], but their effects on phytopathogens remain unclear. To clarify this, we first treated *F. graminearum*, *Magnaporthe oryzae* (the causal agent of rice blast) and *Fusarium oxysporum f. sp. cubense* tropical race 4 (FocTR4, the causal agent of Fusarium wilt of banana) with the phenothiazine derivatives chlorpromazine (CPZ) and prochlorperazine (PCZ) (Fig. S1A). As shown in Fig. 1A, the growth of the indicated fungal pathogens were significant reduced under treatments with CPZ and PCZ. Next, we examined the potential effects of these phenothiazines on the fungal pathogenicity. Notably, when treated with CPZ and PCZ, *F. graminearum*, FocTR4 and *M. oryzae* all displayed serious defects in their invasive growths and

virulence on wheat coleoptiles, banana and rice leaves, respectively (Fig. 1B, C and D). We further treated the host plants with these phenothiazines to investigate whether the drugs exert any impacts on the plant development. As shown in Fig. S1B, treatments with these inhibitors have no obvious effects on the development of the host plants. Overall, we conclude that phenothiazine treatment perturbs phytopathogenic fungal development and host invasion.

Phenothiazines target FgVps1 to compromise *F. graminearum* development and pathogenicity

A previous study indicated that phenothiazines target dynamin to inhibit endocytosis [40]. We therefore used the endocytic marker dye FM4-64 to stain *F. graminearum* and monitor the impact of the substances on endocytosis efficiency. We found that internalization of FM4-64 was significantly reduced under phenothiazines treatment, suggesting the conserved impact of phenothiazines on endocytosis in *F. graminearum* (Fig. 2A, Fig. S2A). We also observed that the pathogenicity of *F. graminearum* on wheat heads was also reduced following treatments with the endocytic inhibitors (Fig. S2B). We further conducted a phylogenetic analysis to identify the potential dynamin target proteins in *F. graminearum*. As shown in Fig. 2B, FgVps1(FGSG_07172) is the only member of the dynamin family of proteins that is involved in endocytic vesicle scission. To test the role of FgVps1 in endocytosis, we generated Δ*Fgvps1* mutant and confirmed the gene deletion by Southern blot assay (Fig. S2C). Consistent with phenothiazine treatment, loss of *FgVPS1* impaired the internalization of FM4-64 into the vacuole, indicating the importance of FgVps1 in endocytosis efficiency in *F. graminearum* (Fig. 2C). To further explore the biological functions of FgVps1, we generated a complemented strain Δ*Fgvps1*-com by expressing a vector harboring GFP-*FgVPS1* into the Δ*Fgvps1* mutant (Fig. S2D). Phenotypic analyses revealed that FgVps1 is important for hyphal and conidial morphogenesis, sexual reproduction and virulence of the wheat head blight fungus (Fig. S2 E to G). These results demonstrate that, similar to phenothiazines treatment, FgVps1 loss-of-function perturbs *F. graminearum* development and pathogenicity.

To investigate the relationship between the phenothiazines treatment and FgVps1 GTPase activity, we purified a GST-FgVps1 recombinant protein and determined its GTPase activity in the presence/absence of phenothiazines. It was observed that the GTPase activity of FgVps1 was

significantly reduced under the phenothiazines treatment, compared to the untreated reaction system (Fig. 2D). Next, we used molecular docking approach (AutoDock [43]) to unveil the possibility of interaction between FgVps1 and the phenothiazines CPZ and PCZ. Interestingly, we found that CPZ and PCZ share the same binding pocket on FgVps1, which involves the amnio acids ranging from D239 to I247 (Fig. 2E). Structurally, FgVps1 possesses three domains: G (GTPase) domain, DM (dynamin central region) domain and GED (dynamin GTPase effector domain) (Fig. S3A). Through domain mutation, we found that all these domains contribute to the full functions and subcellular distribution of FgVps1 (Fig. S3B and S3C). The phenothiazines binding pocket fall within the G domain which is involved in guanine nucleotides binding and hydrolysis [39]. To validate whether the binding pocket contributes to FgVps1 GTPase activity, we deleted the residues that constitute the binding pocket (D239 to I247) and obtained FgVps1$^{\Delta POC}$ mutant expressing the truncated protein. Next, we purified GST-FgVps1$^{\Delta POC}$ recombinant protein and analyzed its GTPase activity using a GTPase activity assay kit. As shown in Fig. 2F, the binding pocket mutation results in significant reduction in FgVps1 GTPase activity. In addition, the deletion of the binding pocket also hampers the efficiency of endocytosis in *F. gramienarum* (Fig. 2G). Similar to the G domain mutation, loss of the phenothiazines binding pocket impairs the full function and subcellular localization of FgVps1, with the FgVps1 punctate localization detected in the cytosol (Fig. S3 and Fig. 2H and 2I). Taken together, these results suggest that phenothiazines target the dynamin FgVps1 to inhibit its GTPase activity, thereby compromising endocytosis and pathogenicity of *F. graminearum*.

FgVps1 regulates the scission of retromer and sorting nexins coated vesicles

Endocytic cargos enter the endolysosomal pathway to the endosomes where their fates are determined [5]. Since our earlier results identified FgVps1 as the target of phenothiazines (Fig. 2), we decided to further dissect the mechanism of FgVps1-dependent endocytosis in relation to the fungal development and pathogenicity. Therefore, we conducted GFP pull-down tandem LC-MS/MS mass spectrometry to identify potential FgVps1-associated proteins in *F. graminearum*. As shown in Fig. 3A and Table S3, the various proteins involved in endolysososmal sorting were captured and identified, including Rab GTPases, the retromer complex and sorting nexins. In *F. graminearum*, the retromer complex and sorting nexins (FgSnx4-FgSnx41) both contribute to endosomal

trafficking and are required for the fungal development and pathogenicity [11, 12]; but their association with the dynamin FgVps1 remain has not been established. Through time-lapse imaging and co-immunoprecipitation (Co-IP) assays, we found that FgVps1 is closely associated with the retromer and sorting nexins *in vivo* (Fig. S4A and S4B). Previously, the Vps1 was reported to mediate the scission of endosomal tubules in yeast [44, 45]. This prompted us to hypothesize that FgVps1 contributes to the scission of retromer- and sorting nexins-associated tubules in *F. graminearum*. To test this, we transformed FgSnx4-GFP and FgVps35-GFP (the core retromer subunit) vectors into the wild type and Δ*Fgvps1* mutant. In the wild type, the fusion proteins displayed punctate localization predominantly along the plasma membrane (Fig. S4C). In the Δ*Fgvps1* mutant, however, the fluorescence signals were trapped in some tubules in the cytosol, suggesting the involvement of FgVps1 in the scission of retromer- and sorting nexins-associated tubules.

In yeast, the retromer and Snx4-Snx41 dimer mediate distinct recycling pathways [44, 46, 47]. Also, our previously studies showed that the retromer and Snx4-Snx41 dimer both contribute to the recycling of the v-SNARE Snc1 in *M. oryzae* and *F. graminearum* [11, 14, 48]. Further analysis of our FgVps1, FgVps35 and FgSnx4 pull-down data revealed that FgVps35 and FgVps1 have many potential interacting partners in common (Fig. S4D). Thus, we hypothesized that FgVps35 and FgSnx4 may interact to jointly execute their biological functions. To verify this hypothesis, yeast two-hybrid and Co-IP assays were carried to check for possible interaction between FgVps35 and FgSnx4. As shown in Fig. S4E and S4F, FgVps35 directly interacts with FgSnx4 both *in vivo* and *in vitro*. Consistently, co-expression of FgVps35-GFP and FgSnx4-mCherry the in wild type and Δ*Fgvps1* mutant showed close association of FgVps35 and FgSnx4, and both fusion proteins are trapped in the same tubules in the Δ*Fgvps1* mutant (Fig. 3B). To further validate the association of FgVps35 and FgSnx4, in silico interaction model of FgVps35 and FgSnx4 was analyzed using AlphaFold Multimer. As shown in Fig. 3C, N383 residue of FgVps35 was observed to interact with E373 residue of FgSnx4 via hydrogen bonding. To validate this prediction, we disrupted this hydrogen bond by introducing N383A and E373A point mutations in FgVps35 and FgSnx4, respectively, and then analyzed the mutated proteins for possible interaction by yeast two-hybrid assay. We found that the interaction of FgVps35 with FgSnx4 was obviously weakened by N383A mutation but completely abolished by E373A mutation (Fig. 3D). Moreover, pathogenicity tests on wheat heads

revealed that the FgSnx4 E373A mutation causes reduced virulence compared to the wild type (Fig. 3E). These results suggest that FgSnx4 E373 residue is critical for the interaction of FgSnx4 with FgVps35.

FgVps1 is recruited to the endosome by FgRab51 and FgRab7 to engage in endolysosomal sorting

In addition to the retromer and sorting nexins identified, the Rab GTPases FgRab51 and FgRab7 were also repeated captured in our FgVps1 pulldown. By co-expressing mCherry-FgVps1 with GFP-FgRab51 and GFP-FgRab7, we found that FgVps1 partially co-localized with the early endosomal marker FgRab51 but completely co-localized with FgRab7-marked late endosomes and vacuoles. Moreover, Co-IP assays indicated that FgVps1 positively interacts with FgRab51 and FgRab7 *in vivo* (Fig. 3F and 3G). In yeast, Mvp1 was shown to recruit Vps1 to the endosomes, while in *F. graminearum*, Δ*Fgmvp1* mutant showed phenotypic differences with Δ*Fgvps1* [46, 49]. Also, Rab GTPases are required for the recruitment of retromer and sorting nexins to the endosomes [11, 14, 41, 50]. Therefore, we proposed that FgRab51 and FgRab7 could mediate the recruitment of FgVps1 to the endosomes in *F. graminearum*. We checked the localization of GFP-FgVps1 in the wild type, Δ*Fgrab51* and Δ*Fgrab7* mutants. As shown in Fig. 3H, loss of the Rab GTPases resulted in mis-localization of GFP-FgVps1 into the cytosol. We therefore conclude that FgVps1 is recruited to the endosome by FgRab51 and FgRab7 to facilitate the scission of endosomal tubules for retrograde trafficking in *F. graminearum* (Fig. 3I).

Inhibiting the GTPase activity of FgVps1 by phenothiazine treatment causes mis-sorting of Snc1

Given that recruitment of FgVps1 to endosomes is required for effective scission of FgVps35 and FgSnx4 endosomal tubules, and that FgVps35 and FgSnx4 are both required for the recycling of FgSnc1 (Fig. 3, Fig. S4) [11, 48], we reasoned that FgSnc1 recycling could also be required for the functioning of FgRab51, FgRab7 and FgVps1. First, we transformed GFP-FgSnc1 into the wild type and Δ*Fgrab51* and Δ*Fgrab7* mutants and checked for possible alteration in FgSnc1 localization. We found that the plasma membrane localization of FgSnc1 was significantly compromised in the Rab GTPase mutants (Fig. S5A), indicating that the recycling of FgSnc1 also depends on the Rab

GTPases in *F. graminearum*. Next, we investigated the role of FgVps1 in FgSnc1 recycling. Similar to FgVps35 and FgSnx4, FgVps1 can also interact with FgSnc1, and loss of FgVps1 has a severe impact on the trafficking of FgSnc1 back to the plasma membrane (Fig. S5B and S5C).

Our earlier results showed that phenothiazines inhibit FgVps1 GTPase activity, and FgVps1-dependent endosomal tubule scission is required for FgSnc1 sorting (Fig. 2, Fig. S5). It is therefore possible that FgSnc1 recycling would be disrupted under phenothiazine treatments in *F. graminearum*. First, we co-transformed GFP-FgSnc1 with mCherry-FgVps1 and mCherry-FgVps1$^{\Delta POC}$ into Δ*Fgvps1* mutant to monitor the dynamics of FgSnc1, FgVps1 and the GTPase-deficient form of FgVps1. We noticed that the mutation of the phenothiazine binding pocket altered the localization of FgSnc1 (Fig. 4A and Fig. S6A). We further transformed GFP-FgSnc1 into the wild type, Δ*Fgvps1* and Fgvps1$^{\Delta POC}$ mutants and analyzed its localization in these strains. We found that the proportion of FgSnc1 detected on the plasma membrane was significantly low in the Δ*Fgvps1* and Fgvps1$^{\Delta POC}$ mutants (Fig. 4B, Fig. S6B). Similarly, degradation level of FgSnc1 also increased in the Δ*Fgvps1* and Fgvps1$^{\Delta POC}$ mutants following analysis by western blot (Fig. 4C). These results indicate that the GTPase activity is required for the localization of FgSnc1 on plasma membrane. We also found that the reduced GTPase activity of FgVps1 negates the scission of retromer- and sorting nexin-coated endolysosomal tubules (Fig. S6C). Given that phenothiazines inhibit FgVps1 GTPase activity, and considering the conserved role of SNARE Snc1 in the development and pathogenicity of fungal pathogens (Fig. 1 and Fig. 4D), it is possible that Snc1 might be a downstream target of phenothiazines in phytopathogens. We tested this by treating the strains expressing GFP-labeled Snc1 with CPZ and PCZ to evaluate the effects of the phenothiazines on Snc1 proteins distribution. As shown in Fig. 4E, treatment with phenothiazines changed the distribution of Snc1 in the different fungal pathogens. Overall, these results indicate that phenothiazines inhibit the GTPase activity FgVps1 and causes mis-sorting of Snc1, which consequently compromised phytopathogenic fungal development and host infection.

Discussion

During pathogen-host interactions, pathogens exploit the endolysosomal network to fine-tune

283 intracellular homeostasis, thereby facilitating host colonization [9, 10, 11, 12, 13, 14, 15, 16, 17, 18, 19, 20, 21, 22, 23,
284 24, 25, 26, 27, 28, 29, 30]. However, the complex interplay within the endolysosomal network and its
285 potential in fungal disease control remain largely unknown. Here, we identified the endocytic
286 dynamin Vps1 as a key regulator of endolysosomal network in phytopathogens. FgVps1 participates
287 in endocytic trafficking process through association with Rab GTPases, retromer and sorting nexins.
288 Inhibition of FgVps1 by phenothiazine treatments disrupts endocytosis and vesicle trafficking
289 efficiency, which impairs the development and pathogenesis of phytopathogens. (Fig. 5). These
290 results offer novel insights into the mechanism of how endolysosomal network functions, and
291 provide a potentially effective pathogenic fungal control strategy by disrupting endocytic dynamin
292 through repurposing of phenothiazines.
293
294 Phenothiazines, the clinically used antipsychotic drugs, also display antimicrobial effects against
295 human pathogenic bacterial and fungi [51, 52, 53]. Although the mechanisms of phenothiazines activity
296 have been described [52], the underlying mechanism of its antifungal effect remains unclear. Here, we
297 showed that phenothiazines displayed broad-spectrum inhibition against phytopathogens. (Fig. 1).
298 Our results indicated that phenothiazines can interact with the dynamin FgVps1 (through binding to
299 amino acids from D239 to I247 residues of the FgVps1 G domain) to inhibit its GTPase activity,
300 resulting in endocytosis inhibition in *F. graminearum* (Fig. 2). In addition, FgVps1-dependent
301 endocytic trafficking of FgSnc1 was also disrupted under phenothiazine treatments, and this effect
302 is conserved among plant pathogenic fungi (Fig. 4). These results suggest that the anti-fungal effect
303 of phenothiazines can be associated with endolyssosomal network dysfunction. Additionally, we
304 noticed that at a high concentration (100 μg/mL), phenothiazines cause more severe phenotypic
305 defects in the fungi than *FgVPS1* deletion (Fig. 1, Fig. 2 and Fig. S2). Previous studies indicated
306 that phenothiazines cause side effects related to impairment of calcium-calmodulin system,
307 membrane stabilization and efflux pumps [54, 55]. It is possible that these effects also contribute to the
308 antifungal property of phenothiazines. Since phenothiazines are synthetic drugs with diverse
309 biological activities [51], further understanding their mechanism of action may provide an avenue for
310 drug development and repurposing.
311
312 The integrity and functionality of endolysosomal network are vital for successful microbial infection

313 [56, 57, 58]. Additionally, pathogens can manipulate the host's endolysosomal network to enhance their
314 colonization efficiency [57, 59, 60, 61]. Given the importance of endocytosis in endolysosomal network,
315 its inhibition could be a novel approach for the control of fungal pathogens. To date, various
316 inhibitors of endocytosis have been characterized [35, 40]. Among them, phenothiazines were shown
317 to target dynamin GTPase activity in mammals [40]. Here, we provide evidence that the
318 phenothiazines CPZ and PCZ exert the conserved role of inhibiting dynamin GTPase activity, which
319 also broaden our understanding of how the dynamin FgVps1 function in the endolysosomal system
320 in fungal pathogens (Fig. 2, Fig. 3 and Fig. S4). Interestingly, although phenothiazines displayed
321 significant impacts on fungal pathogens, short-term treatment with the drugs does not affect the host
322 plant's growth and development (Fig. S1). However, one of the limitations of the study is our
323 inability to analyze the effects of long-term treatment on the hosts and field experiment.
324
325 Dynamins are multi-domain GTPases that are involved in multiple membrane remodeling
326 (including scission and fusion of endocytic vesicles and organelles) and cell division events [38, 39, 62].
327 Unlike the various dynamin proteins identified in mammals and plants [38, 39], fungi contain three
328 dynamin proteins namely Dnm1, Vps1 and Sey1; Dnm1-dependent mitochondrial fission and Sey1-
329 mediated ER fusion have been shown to be important for development, fungicide resistance and
330 pathogenicity in phytopathogens [63, 64, 65]. Although studies have implicated Vps1 in endocytosis,
331 vesicle scission and peroxisome fission and recycling events [44, 45, 46, 66, 67, 68], the mechanism of its
332 functions in fungal phytopathogens remains largely unknown. Our results showed that, in addition
333 to its role in endocytosis, FgVps1 can be recruited to endosomes by Rab GTPases to mediate
334 endosomal tubule scission, which further facilitates the intracellular trafficking of FgSnc1 (Fig.3,
335 Fig. S5 and Fig. 5). Disruption of FgVps1, either by gene deletion or phenothiazine treatments,
336 significantly impaired the development and pathogenicity of *F. graminearum* (Fig. 2, Fig. S2).
337 Interestingly, unlike the precise organization in yeast and mammals, the endosomal network in
338 fungal pathogens appears to be 'coarse' but efficient. Through the tight interconnection among
339 endolysosomal components, Rab GTPases (Rab5 and Rab7), dynamin (FgVps1) and sorting
340 machineries (retromer and sorting nexins), the endocytic trafficking required for the host
341 colonization process in phytopathogenic fungi can be fine-tuned (Fig. 3 and Fig. S4) [11, 41, 46, 49, 69].
342 Pathogens might have developed this for effective host colonization during long-term co-evolution

with their hosts. As endocytic dynamin is conserved among fungi (Fig. 2) [39], inhibition of endocytic dynamin may act as an effective fungal control strategy.

Materials and methods

Fungal strains and culture conditions

For *F. graminearum*, the PH-1 strain was used as the wild type. For *M. oryzae and F. oxysporum*, 70-15 strain and FocTR4 strains were used as the wild type, respectively. A list of all the strains used in this study is provided in Table S1.

In brief, the culture condition of *F. graminearum* were performed based on previously described [10]. *F. graminearum* strains were cultured on CM, CMC and TBI media for growth, conidial production and DON induction, respectively. For vegetative growth and conidial production assays of *M. oryzae*, the wild-type strain 70-15 was cultured on complete medium as previously described [70]. For *F. oxysporum* growth and conidial production, wild type strains FocTR4 was culture on CM or PDB media as previously descripted [71].

Generation of the *FgVPS1* deletion mutants and complementation

For the generation of Δ*Fgvps1* mutants, split-marker approach was utilized as described previously [70]. Briefly, approximately 1kb upstream and downstream sequences of *FgVPS1* gene were amplified using specific primers in Table S2. The resulting fragments were then fused with hygromycin resistance gene cassette through splicing by overlap extension (SOE) PCR and then transformed into the wild type PH-1 protoplasts. The resulting transformants were further screened by PCR and southern blot assay. For Δ*Fgvps1* complementation, the GFP-Fgvps1 vector was transformed into the Δ*Fgvps1* protoplasts and then the positive transformants were screened using confocal microscopy. Additionally, the selected transformants were further verified through phenotypic assays.

Plant infection assays

For *F. graminearum* infection on wheat coleoptiles, conidia suspensions (10^6 spores/mL) of the indicated strains were inoculated on wheat coleoptiles for 7 days as previous descripted [72]. For

pathogenicity on wheat heads, mycelial plugs of the related strains were inoculated into flowering wheat heads for 14 days as previously descripted [10]. For the monitor of invasive growth, conidia suspensions were injected into wheat coleoptiles and incubated at 28 ℃ in dark with proper humidity for 3 days and then observed under confocal microscopy.

For *M. oryzae* pathogenicity on barley, 10 μL conidial suspension (5×10^4 conidia/mL) of the indicated strains were inoculated on barley leaves for 5 days. For rice spray assay, 10 mL conidial suspensions (5×10^4 conidia/mL) were sprayed on rice 3-week-old CO39 rice seedlings and then incubated at 28 ℃ with high humidity, lesions were recorded at 7 dpi (day post inoculation). For the monitor of invasive growth, the mixture of conidial suspension and phenothiazines were injected into rice leave sheath for 36 h.

For *F. oxysporum* host infection, hyphal blocks of the wild type were inoculated on wound banana leaves with phenothiazines for 3 days, DMSO was used as control. Visualization of invasive growth was performed as previously described [71].

Confocal microscopy

For monitoring endocytosis, conidia of the fungal strain were incubated with 10 μg/mL FM4-64 dye (Cat. T3166, Invitrogen, Carlsbad, California) for 1 min, 10 min, and 25 min, respectively. For staining the plasma membrane, hyphae of the indicated strains were stained with FM4-64 for 1 min and then observed under confocal microscopy. Confocal examination was performed using a Nikon CSU-W1 spinning disk confocal microscope (Nikon, Japan). The excitation and emission wavelengths used were 488 nm/500-550 nm for GFP and 561 nm/570-620 nm for mCherry as previously descripted [14].

Immunoprecipitation-mass spectrometry

For the immunoprecipitation-mass spectrometry assays, wild type strain PH-1 and strains expressing the GFP and GFP-FgVps1 were cultured in liquid CM for two days. Mycelia were harvested, ground into a fine powder, and then incubated in lysis buffer containing 2 mM PMSF and protease inhibitor cocktail (Cat. GRF101, Epizyme Biotech, Shanghai, China) for 30 min. Samples were centrifuged at 12,000 rpm for 20 minutes, and then the total cell lysates were further incubated with 30 μL GFP-Trap A beads (Cat. no. gta-20; ChromoTek Inc., Planegg Martinsried,

403 Germany) for 4 hours and then heated at 100℃ with protein loading buffer (Cat. LT103, Epizyme
404 Biotech, Shanghai, China) for 10 minutes. Finally, the samples were separated by SDS-PAGE and
405 mass spectrometry analysis was conducted to identify the related proteins bound to the GFP-FgVps1.
406
407 **Yeast two hybrid and co-immunoprecipitation (Co-IP) assays**
408 For yeast two hybrid assays, the CDS sequence of the related genes were amplified using the specific
409 primers listed in table S2, the amplified sequences were fused with pGADT7 or pGBKT7 vectors
410 and further verified by sequencing (Sangon biotech, Shanghai, China). The resulting vectors were
411 transformed into yeast strain AH109 according to Matchmaker™ GAL4 Two-Hybrid System 3
412 protocol (Clontech, Mountain View, CA, USA).
413 For Co-IP assay, the strains expressing the fusion proteins were inoculated in liquid CM at 28℃,
414 110 rpm for 36 h. The sampled were collected and ground into fine powder in liquid nitrogen, and
415 then lysed in lysis buffer. The total cell lysates were then incubated with GFP-Trap A beads at 4 ℃
416 for 4 h. The bound proteins were subsequently eluted by heating at 100℃ for 10 min with protein
417 loading buffer and further analyzed by western blot with anti-GFP (Cat. M20004M, Abmart,
418 shanghai, China) and anti-Myc (Cat. ab1326, Abcam, Cambridge, United Kingdom) antibodies.
419
420 **Phylogeny analysis, protein structure modeling and molecular docking**
421 For phylogeny analysis, the proteins sequences of dynamin family proteins were download from the
422 NCBI (https://www.ncbi.nlm.nih.gov/). The related phylogeny tree was constructed using the
423 Neighbor-joining method through MEGA-X and further modified using iTOL [73]. The protein
424 structure of FgVps1, the FgVps35-FgSnx4 multimer were predicted using AlphaFold2 [74] and further
425 visualized using PyMOL. The structures of the prochlorperazine and chlorpromazine were
426 downloaded from the NCBI PubChem and the molecular docking of FgVps1with the
427 prochlorperazine and chlorpromazine were further performed using AutoDock and visualized by
428 PyMOL.
429
430 **Protein purification and GTPase activity assay**
431 For the purification of GST-FgVps1, GST-FgVps1$^{\Delta POC}$ recombinant proteins, the related CDS
432 sequences of FgVps1, FgVps1$^{\Delta POC}$ were amplified using the specific primers listed in Table S2 and

then fused with the pGET-4T-2 vector. The resulting vectors were expressed in *Escherichia coli* BL21 cells and further sonicated in the lysis buffer (150 mM NaCl, 50 mM Tris HCL, pH 8.0, 10% glycerol) containing 2 mM PMSF and protease inhibitor cocktail (Cat. GRF101, Epizyme Biotech, Shanghai, China). After sonication, the suspensions were centrifuged at 4 ℃, 12000rpm for 20 min and incubated with GST beads (Cat. A10018, Abmart, Shanghai, China) for 2 h. The beads were then washed with the lysis buffer and eluted by incubating with the elution buffer (150 mM NaCl, 50 mM Tris HCL, pH 8.0, 150 mM glutathione) at 4 ℃ for 2 h.

For the effects of the phenothiazines on FgVps1 GTPase activity, the purified GST-FgVps1 was incubated with the phenothiazines for 30 min and then the GTPase activity was measured using the GTPase assay kit (Cat. ab272520, Abcam, Cambridge, United Kingdom) and Tristar² S LB 942 multimode reader (Berthold, Germany). For the effects of the pocket mutation on FgVps1 GTPase activity, the purified GST-FgVps1 and GST-FgVps1$^{\Delta POC}$ were quantified using the Bradford Protein Assay Kit (Cat. P0006C, Beyotime, Shanghai, China) and then the GTPase activity were measured using the GTPase assay kit. GST was used as the negative control. Data were collected from three biological repeats.

Author contributions

Conceptualization, Zonghua Wang and Wenhui Zheng; methodology, Xin Chen, Xiaomin Chen and Wenhui Zheng; investigation, Xin Chen, Xiaomin Chen, Yunfei Long and Zhenyu Fang; visualization, Xin Chen, Zonghua Wang and Wenhui Zheng; Writing - Original Draft, Xin Chen; Writing - Review & Editing, Xin Chen, Xiaomin Chen, Yakubu Saddeeq Abubakar, Huawei Zheng, Zonghua Wang and Wenhui Zheng; resources and funding acquisition, Wenhui Zheng.

Acknowledgements

This research was supported by the National Natural Science Foundation of China (32122071, 32272481), and the Natural Science Foundation of Fujian Province (2021J06015). The authors declared no financial or other potential conflict of interest.

References

1. Fones HN, Bebber DP, Chaloner TM, Kay WT, Steinberg G, Gurr SJ. Threats to global food security from emerging fungal and oomycete crop pathogens. *Nat Food* **1**, 332-342 (2020).

2. Dean R*, et al.* The Top 10 fungal pathogens in molecular plant pathology. *Mol Plant Pathol* **13**, 414-430 (2012).

3. van der Does HC, Rep M. Adaptation to the Host Environment by Plant-Pathogenic Fungi. *Annu Rev Phytopathol* **55**, 427-450 (2017).

4. Wang Y, Pruitt RN, Nurnberger T, Wang Y. Evasion of plant immunity by microbial pathogens. *Nat Rev Microbiol* **20**, 449-464 (2022).

5. Cullen PJ, Steinberg F. To degrade or not to degrade: mechanisms and significance of endocytic recycling. *Nat Rev Mol Cell Biol* **19**, 679-696 (2018).

6. Borchers AC, Langemeyer L, Ungermann C. Who's in control? Principles of Rab GTPase activation in endolysosomal membrane trafficking and beyond. *J Cell Biol* **220**, (2021).

7. Migliano SM, Wenzel EM, Stenmark H. Biophysical and molecular mechanisms of ESCRT functions, and their implications for disease. *Curr Opin Cell Biol* **75**, 102062 (2022).

8. Posor Y, Jang W, Haucke V. Phosphoinositides as membrane organizers. *Nat Rev Mol Cell Biol* **23**, 797-816 (2022).

9. Zheng H*, et al.* Rab GTPases are essential for membrane trafficking-dependent growth and pathogenicity in Fusarium graminearum. *Environmental Microbiology* **17**, 4580-4599 (2015).

10. Yang C*, et al.* FgVps9, a Rab5 GEF, Is Critical for DON Biosynthesis and Pathogenicity in Fusarium graminearum. *Front Microbiol* **11**, 1714 (2020).

11. Zheng W*, et al.* The endosomal recycling of FgSnc1 by FgSnx41-FgSnx4 heterodimer is essential for polarized growth and pathogenicity in Fusarium graminearum. *New Phytol* **219**, 654-671 (2018).

12. Zheng W*, et al.* Retrograde trafficking from the endosome to the trans-Golgi network mediated by the retromer is required for fungal development and pathogenicity in Fusarium graminearum. *New Phytol* **210**, 1327-1343 (2016).

13. Wang S*, et al.* The regulatory role of the Aspergillus flavus core retromer complex in aflatoxin metabolism. *J Biol Chem* **298**, 102120 (2022).

14. Chen X, *et al.* Rab7/Retromer-based endolysosomal trafficking is essential for proper host invasion in rice blast. *New Phytologist* **239**, 1384-1403 (2023).

15. Zhang X, *et al.* The small GTPase Ypt7 of Penicillium expansum is required for growth, patulin biosynthesis and virulence. *Food Microbiol* **119**, 104434 (2024).

16. Wu C, *et al.* The retromer CSC subcomplex is recruited by MoYpt7 and sequentially sorted by MoVps17 for effective conidiation and pathogenicity of the rice blast fungus. *Mol Plant Pathol* **22**, 284-298 (2021).

17. Huang LY, Wu M, Yu XY, Li L, Lin FC, Liu XH. Physical interactions and mutational analysis of MoYpt7 in Magnaporthe oryzae. *J Zhejiang Univ Sci B* **19**, 79-84 (2018).

18. Liu J, Lei M, Zhou Y, Chen F. A Comprehensive Analysis of the Small GTPases Ypt7 Involved in the Regulation of Fungal Development and Secondary Metabolism in Monascus ruber M7. *Front Microbiol* **10**, 452 (2019).

19. Li XY, Zhang SP, He L. Retromer subunit, CfVps35 is required for growth development and pathogenicity of Colletotrichum fructicola. *BMC Genom Data* **23**, 68 (2022).

20. Li S, Li X, Li H. The Retromer Subunit CfVps29 Is Involved in the Growth, Development, and Pathogenicity of Colletotrichum fructicola. *J Fungi (Basel)* **8**, (2022).

21. Sun L, *et al.* A Subunit of ESCRT-III, MoIst1, Is Involved in Fungal Development, Pathogenicity, and Autophagy in Magnaporthe oryzae. *Front Plant Sci* **13**, 845139 (2022).

22. Cheng J, Yin Z, Zhang Z, Liang Y. Functional analysis of MoSnf7 in Magnaporthe oryzae. *Fungal Genet Biol* **121**, 29-45 (2018).

23. Xie Q, *et al.* Component Interaction of ESCRT Complexes Is Essential for Endocytosis-Dependent Growth, Reproduction, DON Production and Full Virulence in Fusarium graminearum. *Front Microbiol* **10**, 180 (2019).

24. Xie Q, *et al.* ESCRT-III accessory proteins regulate fungal development and plant infection in Fusarium graminearum. *Curr Genet* **65**, 1041-1055 (2019).

25. Xie Q, *et al.* Endosomal sorting complexes required for transport-0 is essential for fungal development and pathogenicity in Fusarium graminearum. *Environ Microbiol* **18**, 3742-3757 (2016).

26. Sun LX, *et al.* Endosomal sorting complexes required for transport-0 (ESCRT-0) are essential for fungal development, pathogenicity, autophagy and ER-phagy in Magnaporthe oryzae. *Environ Microbiol* **24**, 1076-1092 (2022).

27. Li B, Mao HY, Zhang ZY, Chen XJ, Ouyang SQ. FolVps9, a Guanine Nucleotide Exchange Factor for FolVps21, Is Essential for Fungal Development and Pathogenicity in Fusarium oxysporum f. sp. lycopersici. *Front Microbiol* **10**, 2658 (2019).

28. Zheng W*, et al.* Retromer Is Essential for Autophagy-Dependent Plant Infection by the Rice Blast Fungus. *PLoS Genet* **11**, e1005704 (2015).

29. Liu XH*, et al.* The small GTPase MoYpt7 is required for membrane fusion in autophagy and pathogenicity of Magnaporthe oryzae. *Environ Microbiol* **17**, 4495-4510 (2015).

30. Zheng H*, et al.* Sorting nexin (MoVps17) is required for fungal development and plant infection by regulating endosome dynamics in the rice blast fungus. *Environ Microbiol* **19**, 4301-4317 (2017).

31. Sumarah MW. The Deoxynivalenol Challenge. *J Agric Food Chem* **70**, 9619-9624 (2022).

32. Doherty GJ, McMahon HT. Mechanisms of endocytosis. *Annu Rev Biochem* **78**, 857-902 (2009).

33. Smith SM, Smith CJ. Capturing the mechanics of clathrin-mediated endocytosis. *Curr Opin Struct Biol* **75**, 102427 (2022).

34. Chew HY*, et al.* Endocytosis Inhibition in Humans to Improve Responses to ADCC-Mediating Antibodies. *Cell* **180**, 895-914 e827 (2020).

35. Szewczyk-Roszczenko OK*, et al.* The Chemical Inhibitors of Endocytosis: From Mechanisms to Potential Clinical Applications. *Cells* **12**, (2023).

36. Kaksonen M, Roux A. Mechanisms of clathrin-mediated endocytosis. *Nat Rev Mol Cell Biol* **19**, 313-326 (2018).

37. Mettlen M, Chen PH, Srinivasan S, Danuser G, Schmid SL. Regulation of Clathrin-Mediated Endocytosis. *Annu Rev Biochem* **87**, 871-896 (2018).

38. Ferguson SM, De Camilli P. Dynamin, a membrane-remodelling GTPase. *Nat Rev Mol Cell Biol* **13**, 75-88 (2012).

39. Ramachandran R, Schmid SL. The dynamin superfamily. *Curr Biol* **28**, R411-R416 (2018).

40. Daniel JA*, et al.* Phenothiazine-derived antipsychotic drugs inhibit dynamin and clathrin-mediated endocytosis. *Traffic* **16**, 635-654 (2015).

41. Abubakar YS*, et al.* FgRab5 and FgRab7 are essential for endosomes biogenesis and non-redundantly recruit the retromer complex to the endosomes in Fusarium graminearum. *Stress Biology* **1**, (2021).

42. Simanjuntak Y, Liang JJ, Lee YL, Lin YL. Repurposing of prochlorperazine for use against dengue virus infection. *J Infect Dis* **211**, 394-404 (2015).

43. Morris GM*, et al.* AutoDock4 and AutoDockTools4: Automated docking with selective receptor flexibility. *J Comput Chem* **30**, 2785-2791 (2009).

44. Ma M, Burd CG, Chi RJ. Distinct complexes of yeast Snx4 family SNX-BARs mediate retrograde trafficking of Snc1 and Atg27. *Traffic* **18**, 134-144 (2017).

45. Chi RJ, Liu J, West M, Wang J, Odorizzi G, Burd CG. Fission of SNX-BAR-coated endosomal retrograde transport carriers is promoted by the dynamin-related protein Vps1. *J Cell Biol* **204**, 793-806 (2014).

46. Suzuki SW, Oishi A, Nikulin N, Jorgensen JR, Baile MG, Emr SD. A PX-BAR protein Mvp1/SNX8 and a dynamin-like GTPase Vps1 drive endosomal recycling. *Elife* **10**, (2021).

47. Hettema EH. Retromer and the sorting nexins Snx4/41/42 mediate distinct retrieval pathways from yeast endosomes. *The EMBO Journal* **22**, 548-557 (2003).

48. Long Y*, et al.* Golgi-associated retrograde protein (GARP) complex recruits retromer to trans-Golgi network for FgKex2 and FgSnc1 recycling, necessary for development and pathogenicity of Fusarium graminearum. *bioRxiv*, (2023).

49. Lou Y*, et al.* Genome-Wide Characterization of PX Domain-Containing Proteins Involved in Membrane Trafficking-Dependent Growth and Pathogenicity of Fusarium graminearum. *mBio* **12**, e0232421 (2021).

50. Rojas R*, et al.* Regulation of retromer recruitment to endosomes by sequential action of Rab5 and Rab7. *J Cell Biol* **183**, 513-526 (2008).

51. Jaszczyszyn A*, et al.* Chemical structure of phenothiazines and their biological activity. *Pharmacol Rep* **64**, 16-23 (2012).

52. Varga B, Csonka A, Csonka A, Molnar J, Amaral L, Spengler G. Possible Biological and Clinical Applications of Phenothiazines. *Anticancer Res* **37**, 5983-5993 (2017).

53. Grimsey EM, Piddock LJV. Do phenothiazines possess antimicrobial and efflux inhibitory properties? *FEMS Microbiol Rev* **43**, 577-590 (2019).

54. Sharma S, Kaur H, Khuller GK. Cell cycle effects of the phenothiazines: trifluoperazine and chlorpromazine in Candida albicans. *FEMS Microbiol Lett* **199**, 185-190 (2001).

55. Amaral L*, et al.* Phenothiazines, bacterial efflux pumps and targeting the macrophage for

638 enhanced killing of intracellular XDRTB. *In Vivo* **24**, 409-424 (2010).
639
640 56. Shoji JY, Kikuma T, Kitamoto K. Vesicle trafficking, organelle functions, and unconventional
641 secretion in fungal physiology and pathogenicity. *Curr Opin Microbiol* **20**, 1-9 (2014).
642
643 57. Elwell C, Engel J. Emerging Role of Retromer in Modulating Pathogen Growth. *Trends*
644 *Microbiol* **26**, 769-780 (2018).
645
646 58. Abubakar YS, Sadiq IZ, Aarti A, Wang Z, Zheng W. Interplay of transport vesicles during plant-
647 fungal pathogen interaction. *Stress Biol* **3**, 35 (2023).
648
649 59. Cossart P, Helenius A. Endocytosis of viruses and bacteria. *Cold Spring Harb Perspect Biol* **6**,
650 (2014).
651
652 60. Simonetti B, Daly JL, Cullen PJ. Out of the ESCPE room: Emerging roles of endosomal SNX-
653 BARs in receptor transport and host-pathogen interaction. *Traffic* **24**, 234-250 (2023).
654
655 61. Yuen ELH, Shepherd S, Bozkurt TO. Traffic Control: Subversion of Plant Membrane
656 Trafficking by Pathogens. *Annu Rev Phytopathol* **61**, 325-350 (2023).
657
658 62. Antonny B*, et al.* Membrane fission by dynamin: what we know and what we need to know.
659 *EMBO J* **35**, 2270-2284 (2016).
660
661 63. Zhong K*, et al.* MoDnm1 Dynamin Mediating Peroxisomal and Mitochondrial Fission in
662 Complex with MoFis1 and MoMdv1 Is Important for Development of Functional Appressorium
663 in Magnaporthe oryzae. *PLoS Pathog* **12**, e1005823 (2016).
664
665 64. Kang J-b*, et al.* Mitochondrial dynamics caused by QoIs and SDHIs fungicides depended on
666 FgDnm1 in Fusarium graminearum. *Journal of Integrative Agriculture* **22**, 481-494 (2023).
667
668 65. Chong X*, et al.* The Dynamin-Like GTPase FgSey1 Plays a Critical Role in Fungal
669 Development and Virulence in Fusarium graminearum. *Appl Environ Microbiol* **86**, (2020).
670
671 66. Arlt H, Reggiori F, Ungermann C. Retromer and the dynamin Vps1 cooperate in the retrieval of
672 transmembrane proteins from vacuoles. *J Cell Sci* **128**, 645-655 (2015).
673
674 67. Ekal L, Alqahtani AMS, Hettema EH. The dynamin-related protein Vps1 and the peroxisomal
675 membrane protein Pex27 function together during peroxisome fission. *J Cell Sci* **136**, (2023).
676
677 68. Palmer SE*, et al.* A dynamin-actin interaction is required for vesicle scission during endocytosis
678 in yeast. *Curr Biol* **25**, 868-878 (2015).
679
680 69. Wang J, Fedoseienko A, Chen B, Burstein E, Jia D, Billadeau DD. Endosomal receptor
681 trafficking: Retromer and beyond. *Traffic* **19**, 578-590 (2018).

70. Chen X, *et al.* Trehalose Phosphate Synthase Complex-Mediated Regulation of Trehalose 6-Phosphate Homeostasis Is Critical for Development and Pathogenesis in Magnaporthe oryzae. *mSystems* **6**, (2021).

71. Fang Z, *et al.* Two distinct SNARE complexes mediate vesicle fusion with the plasma membrane to ensure effective development and pathogenesis of Fusarium oxysporum f. sp. cubense. *Molecular Plant Pathology* **25**, (2024).

72. Jia LJ, Wang WQ, Tang WH. Wheat Coleoptile Inoculation by Fusarium graminearum for Large-scale Phenotypic Analysis. *Bio Protoc* **7**, e2439 (2017).

73. Letunic I, Bork P. Interactive Tree of Life (iTOL) v6: recent updates to the phylogenetic tree display and annotation tool. *Nucleic Acids Res*, (2024).

74. Mirdita M, Schutze K, Moriwaki Y, Heo L, Ovchinnikov S, Steinegger M. ColabFold: making protein folding accessible to all. *Nat Methods* **19**, 679-682 (2022).

Figure legend

Fig.1 Treatment of phenothiazines impairs the pathogenicity of phytopathogens.

A. Phenothiazines treatment has significant impacts on the fungal growth of the indicated phytopathogens. For evaluating the effects of phenothiazines on fungal growth, mycelial blocks of *F. graminearum*, *F. oxysporum*, and *M. oryzae* were inoculated on complete medium with or without phenothiazines for 2 days, 3 days, and 7 days, respectively. B. Treatment of CPZ and PCZ impaired the host invasion of the *F. graminearum*. For wheat infection, 50 μL conidia suspensions (10^6 spores/mL) of the *F. graminearum* PH-1 strain were inoculated on wheat coleoptiles with or without CPZ or PCZ for 7 days. For the observation of invasive growth, conidia suspensions of *F. graminearum* PH-1 strain expressing GFP were injected into wheat coleoptiles with CPZ or PCZ; DMSO treatment was used as a control. No obvious invasive hyphae were detected at 3 dpi under the treatment of phenothiazines. C. Effects of CPZ and PCZ treatment on *F. oxysporum* invasion. For pathogenicity assays, hyphal blocks were inoculated on wounded banana leaves for 3 days with CPZ or PCZ treatment, respectively. For the observation of invasive growth, conidial suspensions of *F. oxysporum* expressing GFP were co-incubated with banana roots for 3 days and then the cross sections of the banana roots were observed under confocal microscopy. white asterisks indicate the invasion hyphae of the *F. oxysporum*. The invasive hyphae were hardly detectable in phenothiazine-treated banana roots. D. Effects of PCZ and CPZ treatment on *M. oryzae* host invasion. For the pathogenicity of *M. oryzae* on barley leaves, 10 μL conidia suspensions were inoculated on barley leaves with PCZ or CPZ treatment for 5 days. For the rice spray assay, a 10 mL mixture of conidia suspension (at a final concentration of $5*10^4$) with phenothiazines was sprayed on rice leaves, photos were taken at 7 dpi (days post inoculation). DMSO treatment was used as a control. For the monitor of invasive growth, the mixture of conidia suspension with phenothiazines was injected into rice leaf sheaths for 36 h. No invasive hyphae were detected when co-incubated with the phenothiazines CPZ and PCZ at 36 hpi (hours post inoculation).

Fig.2 Phenothiazines inhibit FgVps1 GTPase activity to impair the endocytosis of *F. graminearum.*

A. Effects of phenothiazines (PCZ and CPZ) treatment on the endocytosis of *F. graminearum*. B. Phylogeny analysis of the dynamin family proteins. The phylogenetic tree was constructed using

741 MEGA-X and then modified with iTOL. C. FM4-64 staining to observed the effects of *FgVPS1* on
742 endocytosis. D. Purification of the GST and GST-FgVps1 recombinant protein and subsequent
743 GTPase activity assays. To evaluate the effects of phenothiazines on FgVps1 GTPase activity, 5 μL
744 of the purified GST-FgVps1 was co-incubated with 5 μL of phenothiazines (at a final concentration
745 of 100 μg/mL) for 30 min and then used for GTPase activity assay. E. Molecular docking of the
746 prochlorperazine and chlorpromazine with FgVps1. The molecular docking of FgVps1with the
747 phenothiazines was analyzed using AutoDock and further visualized by PyMOL. FgVps1 is
748 depicted in surface representation (gray), and PCZ and CPZ are depicted in sticks representation. In
749 the right panel, the binding pocket is depicted in lines (salmon), PCZ is represented in blue, and
750 CPZ is represented in light blue. F. Purification of the GST, GST-FgVps1and GST-FgVps1$^{\Delta POC}$
751 recombinant proteins and subsquent GTPase activity assays. The concentration of the purified
752 recombinant proteins was quantified, and then 10 μL of each protein was used for further GTPase
753 activity assay. G. Effects of phenothiazine drugs binding pocket on the endocytosis of *F.*
754 *graminearum*. H. Confocal examination for the localization of GFP-FgVps1 and GFP-FgVps1$^{\Delta POC}$.
755 I. Pathogenicity assay of the binding pocket mutation on wheat heads.
756
757 **Fig. 3 Rab GTPases-dependent FgVps1 recruitment facilitates FgVps1-mediated**
758 **endolysosomal tubule fission in *F. graminearum.***
759 A. GFP-FgVps1 pull down tandem LC-MS/MS assays for the identification of putative FgVps1
760 interacting proteins. B. Confocal examination for the co-localization of FgVps35-GFP with FgSnx4-
761 mCherry in wild type and Δ*Fgvps1* mutant. White boxes indicate the selected area used for time-
762 lapse imaging. C. Putative interacting model of FgVps35 with sorting nexin FgSnx4. FgVps35 is
763 represented in light blue, FgSnx4 is represented in wheat, and the interface is represented in pale
764 green. Black box indicates the enlarged area. Yellow dash represents the hydrogen bond formed
765 between FgSnx4 E373 and FgVps35 N383. D. Yeast two hybrid assay to verify the effects of point
766 mutations on the interaction between FgVps35 and FgSnx4. E. Pathogenicity assays of the point
767 mutation strains on wheat heads. F. Confocal examination and Co-IP assays to verify the interaction
768 between FgVps1 and the Rab GTPase FgRab51.White boxes indicate the area selected for time-
769 lapse imaging. G. Confocal examination and Co-IP assays to verify the interaction between FgVps1
770 and the Rab GTPase FgRab7.White boxes indicate the area selected for time-lapse imaging. H.

771 Effects of the Rab GTPase on the subcellular distribution of FgVps1. I. Diagram represents the roles
772 of dynamin FgVps1 in the endolysosomal network of *F. graminearum*.
773
774 **Fig. 4 Inhibition of GTPase activity by phenothiazine drugs impair the homeostasis of**
775 **SNARE proteins Snc1 in different phytopathogens.**
776 A. Time-lapse imaging for the dynamics of GFP-FgSnc1 with mCherry-FgVps1 and mCherry-
777 FgVps1$^{\Delta POC}$. B. Confocal examination of the effects of the FgVps1$^{\Delta POC}$ mutation on the distribution
778 of FgSnc1. C. Western blot assay for the protein levels of GFP and GFP-FgSnc1 in the indicated
779 strains. D. Pathogenicity assays of the related *SNC1* mutants in different species. For the
780 pathogenicity of the *F. graminearum*, hyphal blocks of the wild type and Δ*Fgsnc1* mutant were
781 inoculated on wheat heads and then photographed at 14 dpi. For the pathogenicity of Δ*Mosnc1*
782 mutant on rice, conidial suspensions of indicated strains were sprayed on three-weeks rice cultivar
783 CO-39 for 7 days. For the pathogenicity assay of the *F. oxysporum,* hyphal blocks of the wild type
784 and Δ*Focsnc1* were inoculated on wounded banana leaves for 3 days. For the observation of
785 invasive growth, conidial suspensions of the wild type and Δ*Focsnc1* mutant expressing GFP were
786 co-incubated with banana roots for 3 days and then the cross sections of the banana roots were
787 observed under confocal microscopy. E. Confocal examination for the effects of phenothiazine
788 drugs treatment on the distribution of Snc1 in phytopathogens. White boxes indicate the enlarged
789 area in the right panel. The plasma membrane and septa were marked by FM4-64 dye.
790
791 **Fig. 5 Proposed model of dynamin FgVps1 in endocytic trafficking and pathogenicity of *F.***
792 ***graminearum*.**
793 For endolysosomal trafficking, the endocytic dynamin FgVps1 engages in the release of the
794 endocytosed vesicles to allow the cell surface cargos to enter the endolysosomal system. Moreover,
795 FgVps1 is recruited to the endosome by Rab GTPases (FgRab51 and FgRab7) to mediate the fission
796 of retromer and sorting nexins endolysosomal tubules, facilitating the recycling of related cargos
797 (e.g., FgSnc1). Dynamin GTPase inhibition, caused by dynamin FgVps1 disruption or
798 phenothiazines treatment, significantly inhibits the endocytosis and endocytic trafficking process,
799 resulting in the dysfunction of the endolysosomal system and leading to defects in host colonization.
800

A

Control
+ DMSO

Chlorpromazine (CPZ)
+ 50 μg/mL
+ 100 μg/mL

Prochlorperazine (PCZ)
+ 50μg/mL
+ 100 μg/mL

F. graminearum (PH-1)

F. oxysporum (FocTR4)

M. oryzae (70-15)

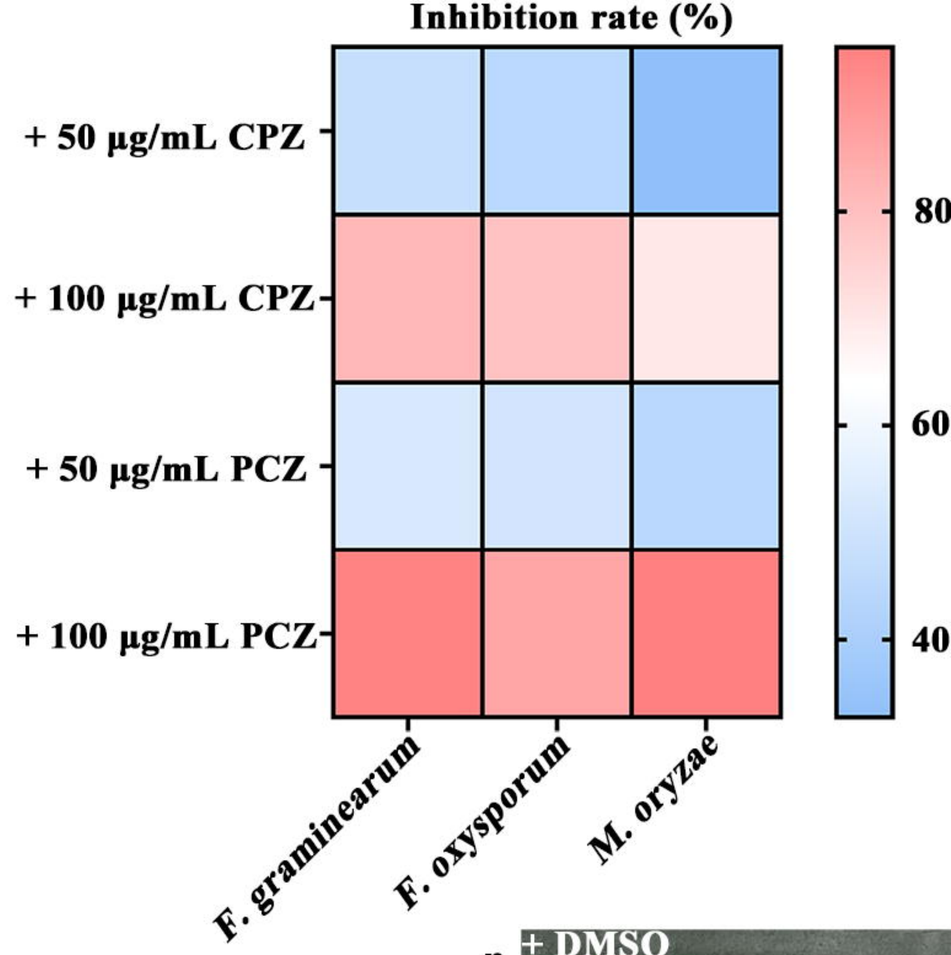

B

Control
+ DMSO

CPZ treatment
+ 50 μg/mL
+ 100 μg/mL

PCZ treatment
+ 50 μg/mL
+ 100 μg/mL

Wheat coleoptiles infection

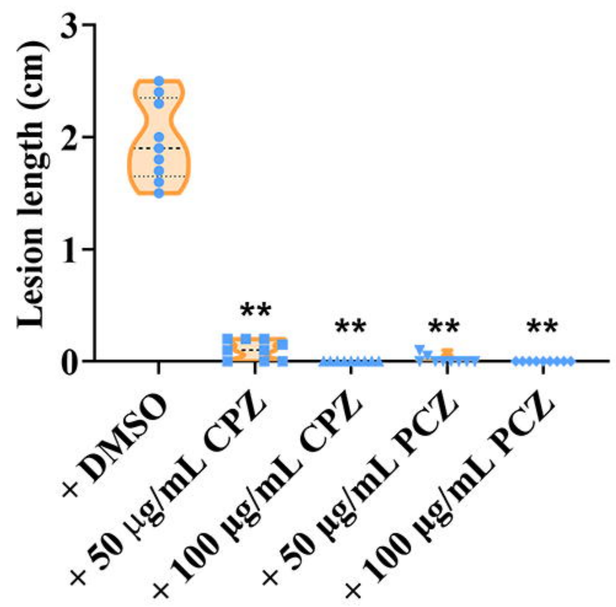

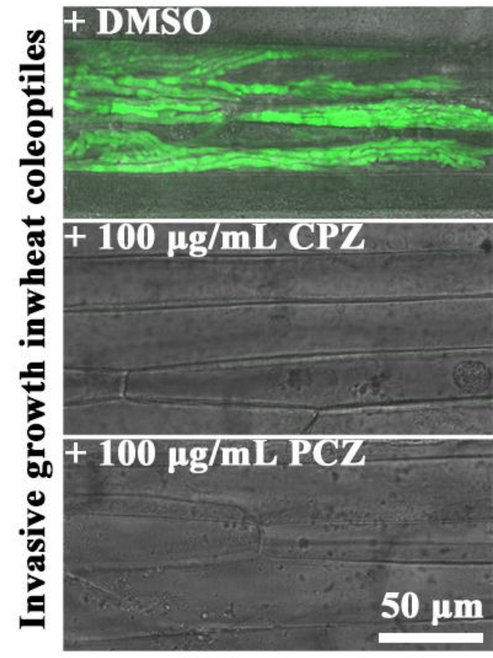

C

Control | CPZ treatment | Control | PCZ treatment

FocTR4 infection on banana leaves

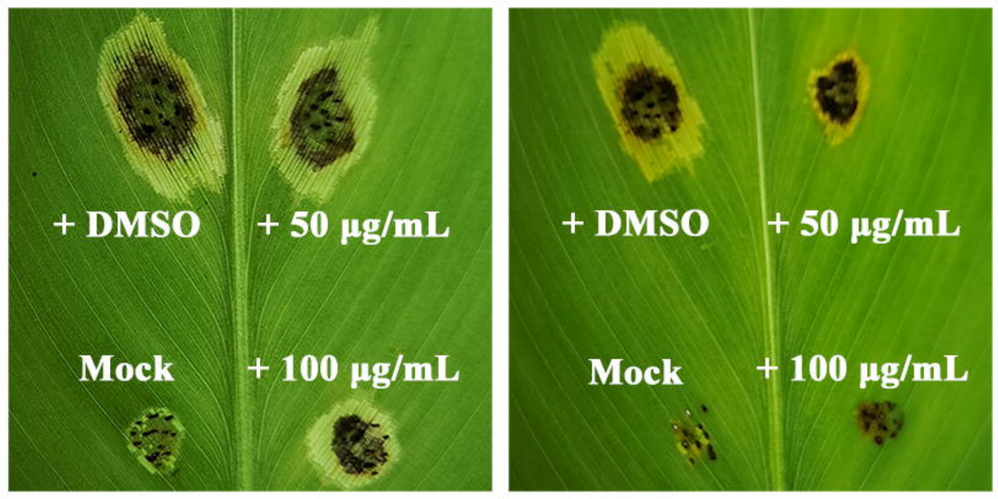

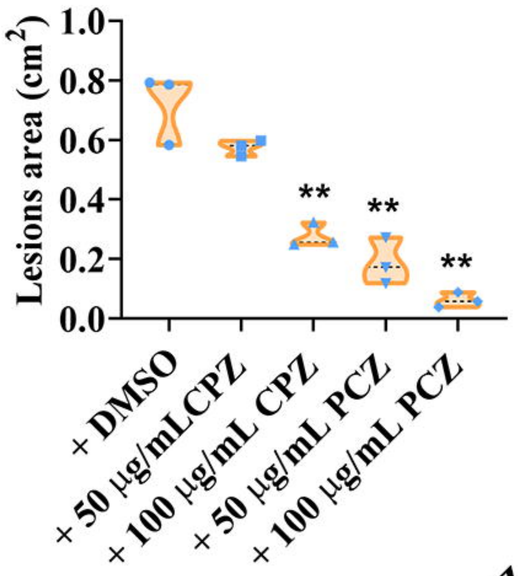

Invasive growth in banana roots

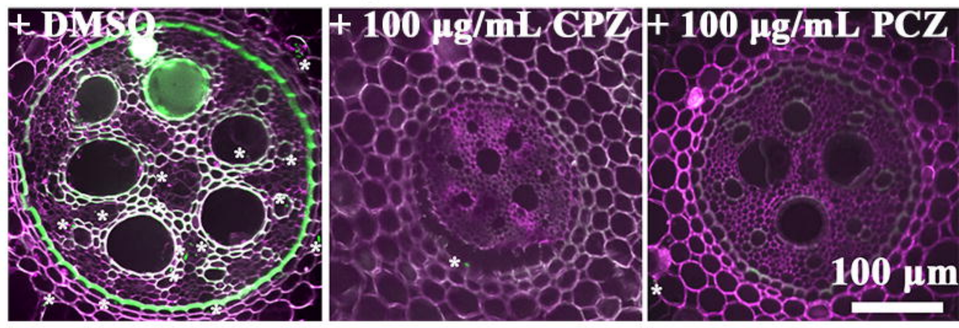

D

CPZ
PCZ

+ DMSO
+ 50 μg/mL
+ 100 μg/mL
+ 50 μg/mL
+ 100 μg/mL

Conidial inoculation on barley

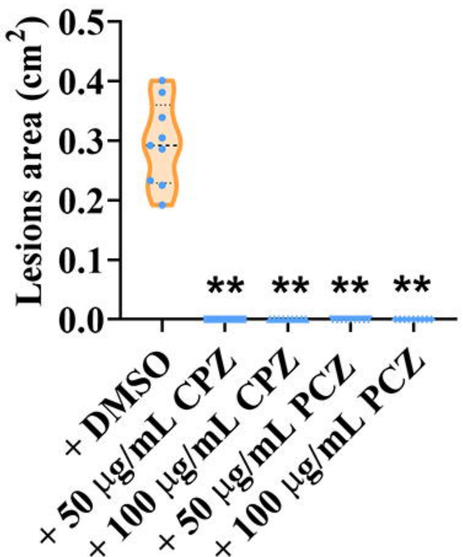

+ DMSO
+ 100 μg/mL CPZ
+ 100 μg/mL PCZ

Rice spray assay

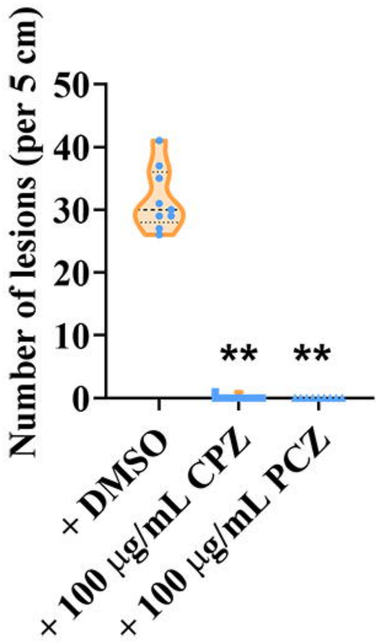

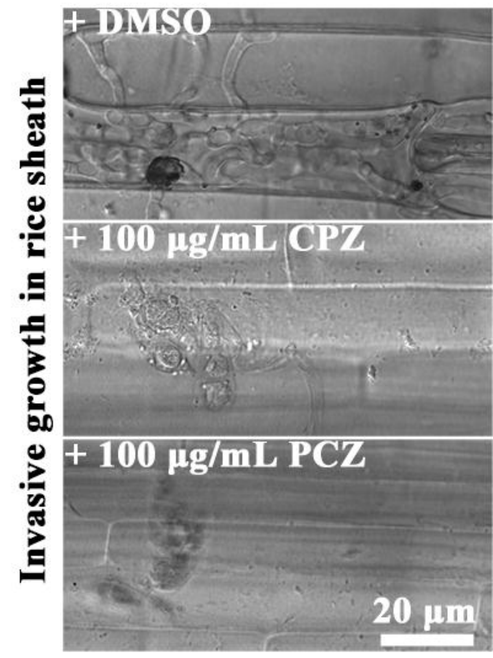

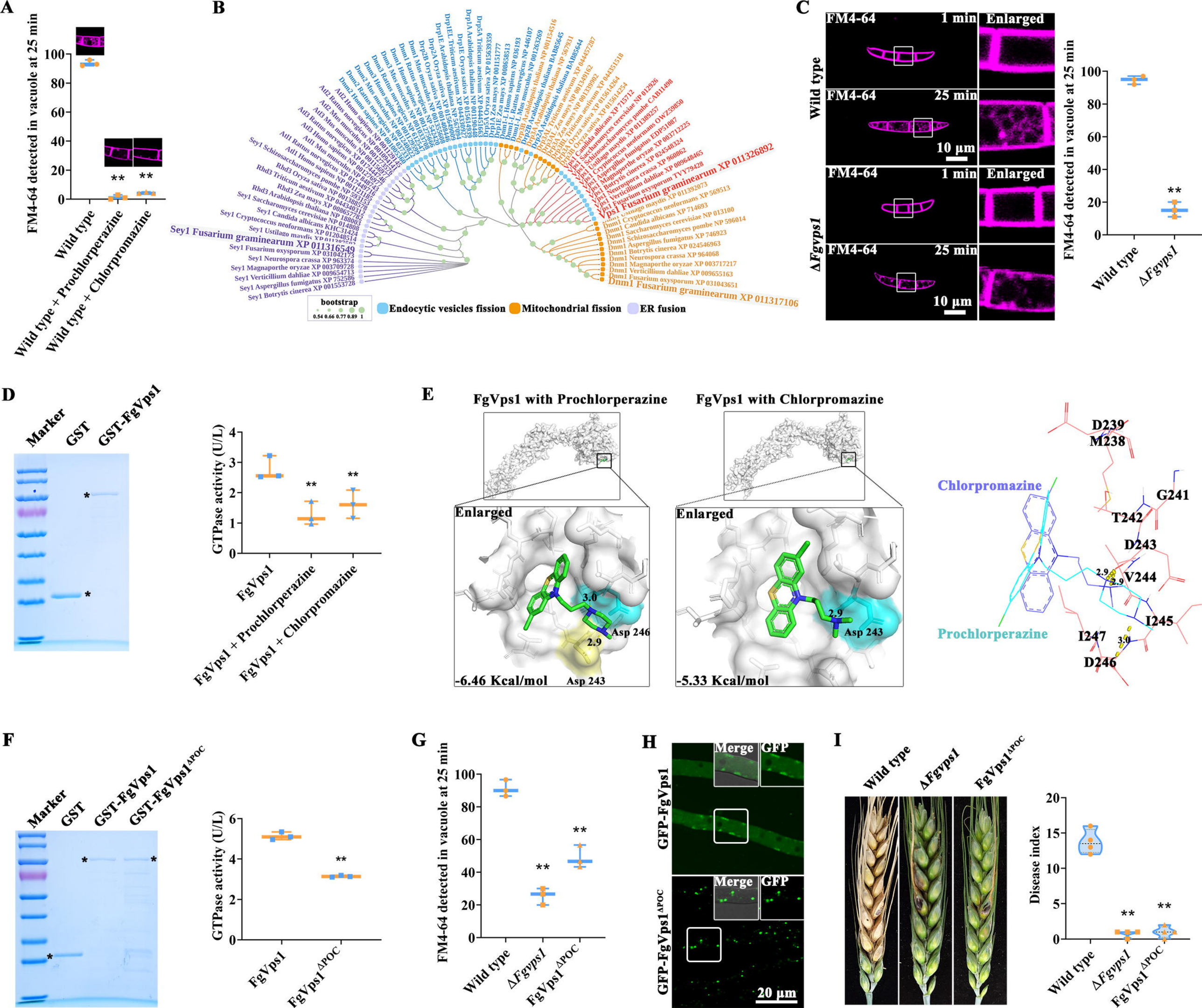
A
FM4-64 detected in vacuole at 25 min
Wild type
Wild type + Prochlorperazine
Wild type + Chlorpromazine
B
Sey1 Fusarium graminearum XP 011316549
Vps1 Fusarium graminearum XP 011326892
Dnm1 Fusarium graminearum XP 011317106
bootstrap
Endocytic vesicles fission
Mitochondrial fission
ER fusion
C
FM4-64
1 min
25 min
Enlarged
10 μm
Wild type
ΔFgvps1
FM4-64 detected in vacuole at 25 min
D
Marker
GST
GST-FgVps1
GTPase activity (U/L)
FgVps1
FgVps1 + Prochlorperazine
FgVps1 + Chlorpromazine
E
FgVps1 with Prochlorperazine
FgVps1 with Chlorpromazine
Enlarged
Asp 246
Asp 243
-6.46 Kcal/mol
-5.33 Kcal/mol
Chlorpromazine
Prochlorperazine
D239
M238
G241
T242
D243
V244
I245
I247
D246
F
GST-FgVps1ΔPOC
G
FM4-64 detected in vacuole at 25 min
Wild type
ΔFgvps1
FgVps1ΔPOC
H
Merge
GFP
GFP-FgVps1
GFP-FgVps1ΔPOC
20 μm
I
Disease index

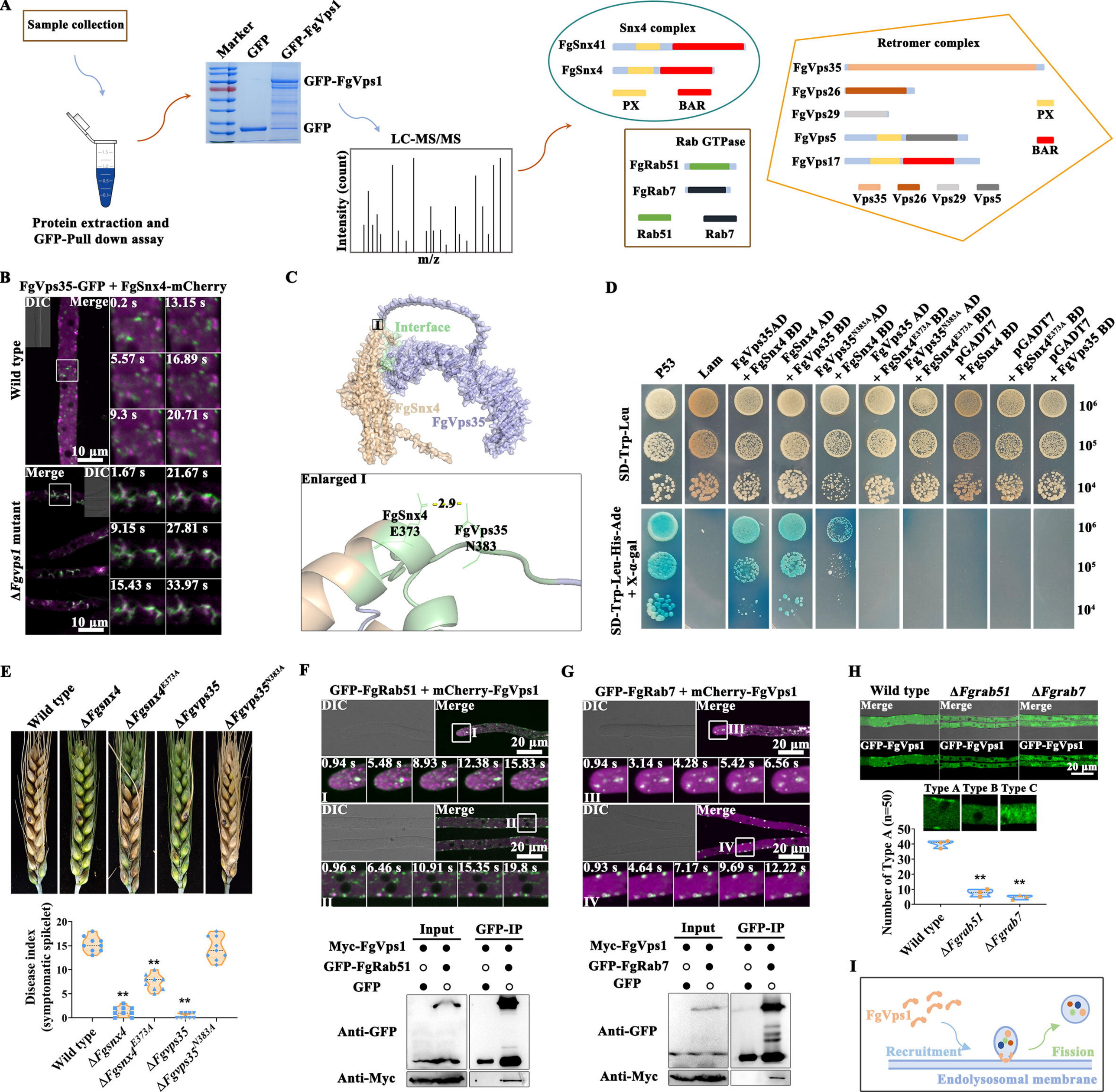
A
Sample collection
Protein extraction and GFP-Pull down assay
Marker
GFP
GFP-FgVps1
GFP-FgVps1
GFP
LC-MS/MS
Intensity (count)
m/z
Snx4 complex
FgSnx41
FgSnx4
PX
BAR
Rab GTPase
FgRab51
FgRab7
Rab51
Rab7
Retromer complex
FgVps35
FgVps26
FgVps29
FgVps5
FgVps17
PX
BAR
Vps35 Vps26 Vps29 Vps5
B
FgVps35-GFP + FgSnx4-mCherry
DIC
Merge
0.2 s
13.15 s
5.57 s
16.89 s
9.3 s
20.71 s
Wild type
10 μm
Merge
DIC
1.67 s
21.67 s
9.15 s
27.81 s
15.43 s
33.97 s
ΔFgvps1 mutant
10 μm
C
Interface
FgSnx4
FgVps35
Enlarged I
2.9
FgSnx4
E373
FgVps35
N383
D
P53
Lam
FgVps35AD + FgSnx4 BD
FgSnx4 AD + FgVps35 BD
FgVps35N383A AD + FgSnx4 BD
FgVps35 AD + FgSnx4E373A BD
FgVps35N383A AD + FgSnx4E373A BD
pGADT7 + FgSnx4 BD
pGADT7 + FgSnx4E373A BD
pGADT7 + FgVps35 BD
SD-Trp-Leu
SD-Trp-Leu-His-Ade + X-α-gal
10⁶
10⁵
10⁴
E
Wild type
ΔFgsnx4
ΔFgsnx4E373A
ΔFgvps35
ΔFgvps35N383A
Disease index (symptomatic spikelet)
Wild type
ΔFgsnx4
ΔFgsnx4E373A
ΔFgvps35
ΔFgvps35N383A
F
GFP-FgRab51 + mCherry-FgVps1
DIC
Merge
20 μm
0.94 s
5.48 s
8.93 s
12.38 s
15.83 s
0.96 s
6.46 s
10.91 s
15.35 s
19.8 s
Input
GFP-IP
Myc-FgVps1
GFP-FgRab51
GFP
Anti-GFP
Anti-Myc
G
GFP-FgRab7 + mCherry-FgVps1
DIC
Merge
20 μm
0.94 s
3.14 s
4.28 s
5.42 s
6.56 s
0.93 s
4.64 s
7.17 s
9.69 s
12.22 s
Input
GFP-IP
Myc-FgVps1
GFP-FgRab7
GFP
Anti-GFP
Anti-Myc
H
Wild type
ΔFgrab51
ΔFgrab7
Merge
GFP-FgVps1
20 μm
Type A
Type B
Type C
Number of Type A (n=50)
Wild type
ΔFgrab51
ΔFgrab7
I
FgVps1
Recruitment
Fission
Endolysosomal membrane

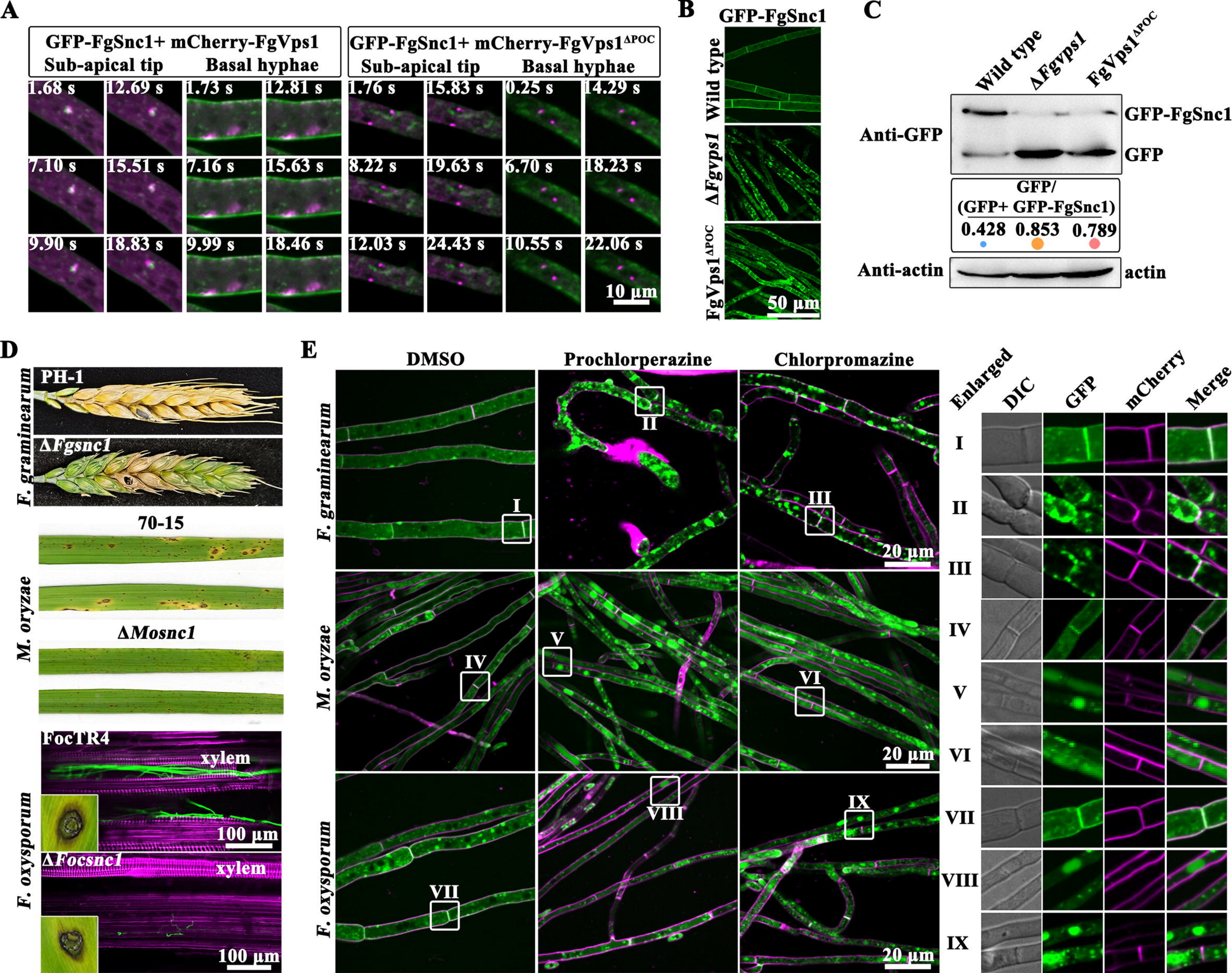
A
GFP-FgSnc1+ mCherry-FgVps1
Sub-apical tip
Basal hyphae
GFP-FgSnc1+ mCherry-FgVps1ΔPOC
Sub-apical tip
Basal hyphae
1.68 s
12.69 s
1.73 s
12.81 s
1.76 s
15.83 s
0.25 s
14.29 s
7.10 s
15.51 s
7.16 s
15.63 s
8.22 s
19.63 s
6.70 s
18.23 s
9.90 s
18.83 s
9.99 s
18.46 s
12.03 s
24.43 s
10.55 s
22.06 s
10 μm
B
GFP-FgSnc1
Wild type
ΔFgvps1
FgVps1ΔPOC
50 μm
C
Wild type
ΔFgvps1
FgVps1ΔPOC
Anti-GFP
GFP-FgSnc1
GFP
GFP/
(GFP+ GFP-FgSnc1)
0.428
0.853
0.789
Anti-actin
actin
D
F. graminearum
PH-1
ΔFgsnc1
70-15
M. oryzae
ΔMosnc1
F. oxysporum
FocTR4
xylem
100 μm
ΔFocsnc1
xylem
100 μm
E
DMSO
Prochlorperazine
Chlorpromazine
F. graminearum
M. oryzae
F. oxysporum
I
II
III
IV
V
VI
VII
VIII
IX
20 μm
Enlarged
DIC
GFP
mCherry
Merge

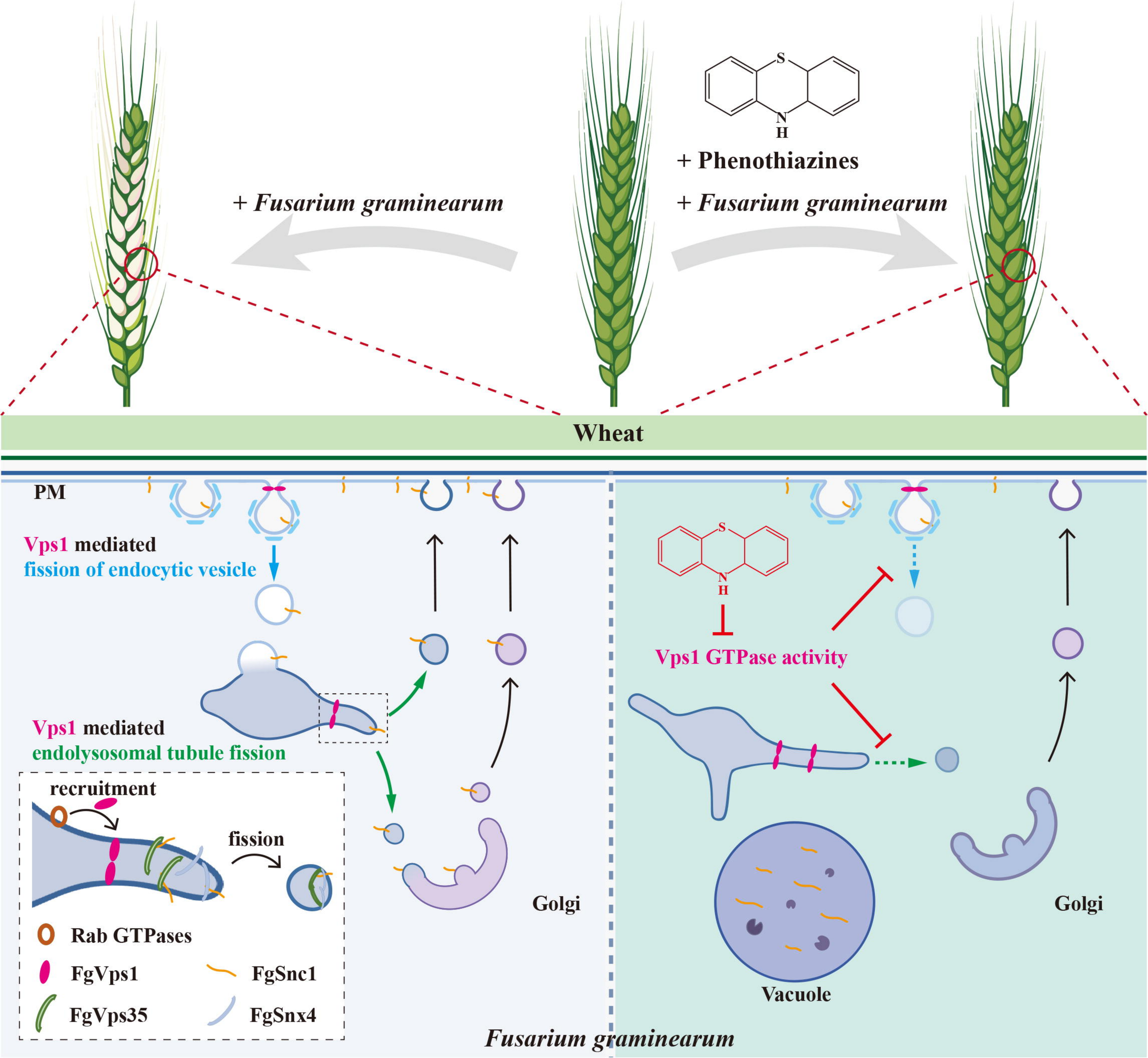
+ Fusarium graminearum
+ Phenothiazines
+ Fusarium graminearum
Wheat
PM
Vps1 mediated
fission of endocytic vesicle
Vps1 mediated
endolysosomal tubule fission
recruitment
fission
Rab GTPases
FgVps1
FgSnc1
FgVps35
FgSnx4
Golgi
Vps1 GTPase activity
Vacuole
Golgi
Fusarium graminearum